

# The complex radio and X-ray structure in the nuclear regions of the active galaxy NGC 1365

Ian R. Stevens<sup>1</sup>, Duncan A. Forbes<sup>1</sup>, Ray P. Norris<sup>2</sup>

<sup>1</sup> School of Physics and Astronomy, University of Birmingham, Edgbaston, Birmingham, B15 2TT, UK

<sup>2</sup> Australia Telescope National Facility, CSIRO, PO Box 76, Epping, NSW 2121, Australia

*irs@star.sr.bham.ac.uk, forbes@star.sr.bham.ac.uk, rnorris@atnf.csiro.au*

Accepted .....; Received .....; in original form .....

## ABSTRACT

We present a multiwavelength analysis of the prominent active galaxy NGC 1365, in particular looking at the radio and X-ray properties of the central regions of the galaxy.

We analyse *ROSAT* (PSPC and HRI) observations of NGC 1365, and discuss recent *ASCA* results. In addition to a number of point sources in the vicinity of NGC 1365, we find a region of extended X-ray emission extending along the central bar of the galaxy, combined with an emission peak near the centre of the galaxy. This central X-ray emission is centred on the optical/radio nucleus, but is spatially extended. The X-ray spectrum can be well fitted by a thermal plasma model, with a temperature of  $kT = 0.6 - 0.8$  keV and a very low local absorbing column. The thermal spectrum is suggestive of starburst emission rather than emission from a central black-hole.

The ATCA radio observations show a number of hotspots, located in a ring around a weak radio nucleus. Synchrotron emission from electrons accelerated by supernovae and supernova remnants (SNRs) is the likely origin of these hotspots (Condon & Yin 1990; Forbes & Norris 1998). The radio nucleus has a steep spectrum, indicative perhaps of an AGN or SNRs. The evidence for a jet emanating from the nucleus (as has been previously claimed) is at best marginal. The extent of the radio ring is comparable to the extended central X-ray source.

We discuss the nature of the central activity in NGC 1365 in the light of these observations. The extended X-ray emission and the thermal spectra strongly suggest that at soft X-ray energies we are not seeing emission predominantly from a central black-hole, although the presence of Fe-K line emission at higher energies does suggest the presence of an AGN. Consequently, a black-hole is probably not the dominant contributor to the energetics of the central regions of NGC 1365 at radio, optical or soft X-ray wavelengths. Activity associated with a starburst is likely the dominant explanation for the observed properties of NGC 1365.

**Key words:** ISM: jets and outflows – galaxies: starburst – galaxies: stellar content – stars: Wolf-Rayet – X-rays: galaxies

## 1 INTRODUCTION

It is becoming clear that in Seyfert galaxies there is a close link between the Seyfert nucleus, which may harbour a super-massive black-hole, and circumnuclear starburst activity. The nature of the connection is unclear, whether the starburst is somehow responsible for the formation or perhaps fuelling of a central black-hole, or whether activity associated with the central black-hole is responsible for triggering the star-formation. To understand the complexities

of the central regions of active galaxies and the relationship between Seyfert and starburst activity we need detailed multiwavelength studies of individual galaxies. In this paper we present such a study of the prominent spiral galaxy NGC 1365, concentrating on X-ray and radio data.

NGC 1365 is classified as a SBb(s)I type barred spiral galaxy by Sandage & Tammann (1981), and is a member of the Fornax cluster. NGC 1365 is an active galaxy with an emission line nucleus (with both broad and narrow H $\alpha$  emission) located at the edge of a dust-lane, which runs

across the central bulge (Véron *et al.* 1980). We adopt a distance of 20 Mpc for NGC 1365 throughout this paper.

The active nucleus of NGC 1365 has been multiply classified. For instance, on the basis of the FWHM of the H $\alpha$  component Hjelm & Lindblad (1996) classified NGC 1365 as a Seyfert 1.5 (see also Kristen *et al.* 1997). Turner, Urry & Mushotzky (1993) classified it as a Seyfert 2, and Maiolino & Rieke (1995) as a Seyfert 1.8.

In addition to the active nucleus, NGC 1365 contains a large number of giant HII regions, with several of them in close proximity to the nucleus (Alloin *et al.* 1981). *HST* Faint Object Camera observations of NGC 1365, discussed by Kristen *et al.* (1997), reveal numerous bright super star-clusters around the nucleus. These clusters are very compact, with radii estimated to be  $\leq 3$  pc, and tend to fall on an elongated ring around the nucleus. Correlations between the locations of these super-star clusters and sources in this paper will be discussed later.

Hjelm & Lindblad (1996) have also discussed optical observations of the central regions of NGC 1365, and in particular the conical region of high excitation gas associated with the nucleus. They describe a kinematical model of this region, whereby gas is accelerated in a bi-conical region, with the cone axes aligned with the galaxy rotation axis. The cone is also aligned with a suggested radio jet (Sandqvist, Jörsäter & Lindblad 1995), though we shall discuss the nature of this jet in more detail later. Radio observations of NGC 1365 by Saikia *et al.* (1994), Sandqvist *et al.* (1995) and Forbes & Norris (1998) reveal a complex, possibly ringlike structure around the nucleus, but with several radio hotspots loosely coincident with the giant HII regions.

One of the nuclear HII regions (region L4 in the terminology of Alloin *et al.* 1981) shows a broad emission line at around 5696Å, due to CIII emission (Phillips & Conti 1992). The strength of this line, and the absence of CIV 5808Å is indicative of the presence of between 350 and 1400 WC9 Wolf-Rayet (WR) stars. The presence of such a substantial population of massive WR stars is indicative of very recent (3 – 6 Myr) star-formation close to the nucleus. NGC 1365 was not included in the original WR galaxy catalogue of Conti (1991), but was included in the subclass of WR barred spiral galaxies by Contini, Davoust & Considère (1995). We shall discuss the properties of NGC 1365 in relation to WR galaxies in Section 4.1.

The nuclear regions of NGC 1365 were seen as a moderately strong IR source with *IRAS* (Ghosh *et al.* 1993). NGC 1365 was also observed as a soft X-ray source by the *EINSTEIN* satellite, with an X-ray luminosity of  $L_x = 8.2 \times 10^{40}$  erg s $^{-1}$  (for the 0.2–4.0 keV waveband, corrected for distance; Fabbiano, Kim & Trinchieri 1992). Komossa & Schulz (1998) have also recently presented a study of the X-ray properties of NGC 1365.

In this paper we present a detailed analysis of radio and X-ray observations of NGC 1365 in an attempt to better understand the puzzling central regions of this galaxy. The X-ray data probe the hot thermal gas from starburst emission and the hard non-thermal radiation from any massive compact object. Radio observations on the other hand allows us to look for non-thermal emission from synchrotron radiation from SNRs or an AGN, or for thermal free-free emission from young stellar populations of HII regions. The

combined X-ray/radio morphology will in turn allow us to investigate the origin of the emission.

NGC 1365 has been observed on several occasions at X-ray energies. Here we shall concentrate on observations with the *ROSAT* satellite (both PSPC and HRI instruments), but also discuss recent results from the *ASCA* satellite. These satellites and instruments have a range of complementary properties - the *ROSAT* PSPC is very sensitive, has reasonable spectral resolution and reasonable spatial resolution ( $\sim 25''$ ), allowing us to probe the spectral properties of central regions and look for any extended emission; the *ROSAT* HRI is less sensitive and has essentially no spectral resolution, but has excellent spatial resolution ( $\sim 5''$ ) allowing a detailed study of the X-ray morphology of NGC 1365. *ASCA* on the other hand has poor spatial resolution (a few arcminutes), but excellent spectral resolution, which coupled with a broader bandpass (0.5 – 10 keV, as compared to 0.1 – 2.4 keV for *ROSAT*) allows us to investigate the spectral properties of the integrated emission from NGC 1365 in more detail. In particular, *ASCA* allows us to look for harder X-ray emission that might be associated with a Seyfert nucleus. Radio observations from the VLA have been previously reported (e.g. Sandqvist *et al.* 1995). Here we use the Australia Telescope Compact Array (ATCA) observations of Forbes & Norris (1998) which gives a more circular beam than the VLA for a galaxy at Dec.  $\sim -36^\circ$ . We report on observations at both 3cm and 6cm.

Some of the important issues that we intend to address in this paper are as follows:

- (i) What is the origin of the X-ray emission from NGC 1365; i.e. is it associated with a massive central black-hole or is it due to starburst activity?
- (ii) What is the origin of the radio hotspot emission?
- (iii) What is the energetic importance of the Seyfert nucleus?
- (iv) Do we find any complimentary evidence for jets, winds, outflows or emission line cones at radio/X-ray frequencies?

The paper is organised as follows; in Section 2 we discuss the X-ray observations of NGC 1365 with the *ROSAT* and *ASCA* satellites, in Section 3 we discuss the ATCA radio data, and in Section 4 we discuss what the radio and X-ray data tell us about the nature of the central activity in NGC 1365.

## 2 X-RAY OBSERVATIONS OF NGC 1365

A summary of the X-ray observations discussed in this paper is given in Table 1. In all cases we create background subtracted images, and use the point source searching (PSS) package (Allan 1993) to search for unresolved sources. Turner *et al.* (1993) have discussed the point sources in the vicinity of NGC 1365 detected with the *ROSAT* PSPC and suggest some plausible candidates, namely X-ray binaries, HII regions in the spiral arms and possibly background AGN (see also Komossa & Schulz 1998). Several of the candidates are embedded in the disk of the galaxy and it is difficult to identify counterparts. Because we have also detected diffuse X-ray emission there is also the possibility that

**Table 1.** A summary of the X-ray and radio observations of NGC 1365 discussed in this paper

Instrument	Date	PI	Duration
X-ray Observations			
ROSAT/PSPC	1992 Aug 22 – Aug 23	T. J. Turner	2.6 ksec
ROSAT/PSPC	1993 Feb 05 – Feb 10	T. J. Turner	6.2 ksec
ROSAT/HRI	1994 Jul 20 – Aug 04	K. P. Singh	9.9 ksec
ROSAT/HRI	1995 Jul 03 – Jul 04	K. P. Singh	9.8 ksec
Radio Observations			
ATCA/6cm	1994 Nov 10 – Nov 11	D. A. Forbes	36 ksec
ATCA/3cm	1994 Nov 10 – Nov 11	D. A. Forbes	36 ksec

some of the HRI sources are merely spurious detections of irregularities in the diffuse emission.

For the *ROSAT* PSPC observations we extracted source spectra for regions around NGC 1365 and fitted them with simple spectral models. More details are given in the appropriate sections below.

The  $z = 0.308$  BL Lac object 1E 0331.3-3629 is in the field of view of all the observations. This X-ray source was discovered by the *EINSTEIN Extended Medium Sensitivity Survey*. The optical identification is discussed in Maccacaro *et al.* (1994). The X-ray properties of 1E 0331.3-3629 are discussed in Lamer, Brunner & Staubert (1996). We have cross checked the position of 1E 0331.3-3629 with the APM catalogue (Irwin 1992), and the optical position is well determined to arcsecond accuracy. We adopt a position of RA = 03 33 12.3, Dec. =  $-36^{\circ} 19' 47''$  (J2000) for 1E 0331.3-3629 (c.f. Maccacaro *et al.* 1994). Consequently we can use the X-ray determined position of 1E 0331.3-3629 to accurately align the X-ray images. This is important as it enables us to accurately define the location of the X-ray emission in NGC 1365, and relate it to the radio emission, and hence understand its origin.

## 2.1 ROSAT PSPC Observations

NGC 1365 has been observed with the *ROSAT* PSPC on two occasions (with an observation length of 2.6 ksec for observation No.1, and 6.2 ksec for observation No.2, with the observations separated by about 6 months). Results from these observations have been reported by Turner *et al.* (1993), who also reported on PSPC observations of 5 other Seyfert 2 galaxies.

Turner *et al.* (1993) found a total of 5 point sources near the nuclear source in NGC 1365, and found that the emission from the nuclear source was not well fitted by an absorbed power-law, but could be better fitted by either a model with a power-law, plus a Raymond-Smith thermal component (with  $kT = 0.6$  keV), or by a power-law with an emission line at an energy of 0.8 keV. It is worth noting that the fit quality for the other Seyfert galaxies, assuming a power-law model, was substantially better than for NGC 1365.

We have reanalysed both *ROSAT* PSPC observations. We extracted background subtracted spectral images for both observations. We adjusted the pointing of both observations using the BL Lac object 1E 0331.3-3629. The X-ray image (Figure 1) shows moderately strong X-ray emis-

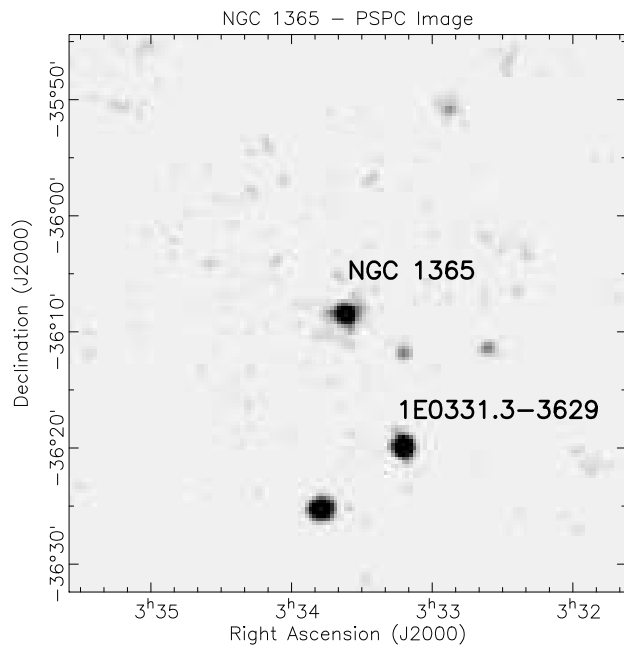


**Figure 1.** The central  $0.8 \times 0.8$  degree region of the *ROSAT* PSPC field containing NGC 1365. This is the longer, 1993 Feb, observation, with an observation length of 6.2 ksec. The X-ray image has been background subtracted, and has been extracted with a  $5''$  pixel size and smoothed with a Gaussian of FWHM  $10''$ . There is strong X-ray emission from NGC 1365, at the centre of the field, along with several other point sources. The strong source to the SW of NGC 1365 is the BL Lac object 1E 0331.3-3629, which is apparent in all the X-ray observations and is used to register the X-ray images. The source to the SE of NGC 1365 is an unclassified object, possibly associated with a faint optical object from the Digital Sky Survey, which is strongly variable, and is extremely weak in the later HRI observations. The detector ring structure of the PSPC is barely visible.

sion from NGC 1365 (the precise location will be discussed in Section 4.2) as well as emission from other sources near the galaxy. The strong source to the SW of NGC 1365 is 1E 0331.3-3629.

In Figure 2, for the longer (6.2 ksec) observation, we show X-ray contours of the emission from NGC 1365 superimposed on an optical image from the Digitized Sky Survey. We also show in Figure 2 the radial profile for the X-ray emission, compared to the Point Spread Function (PSF) for

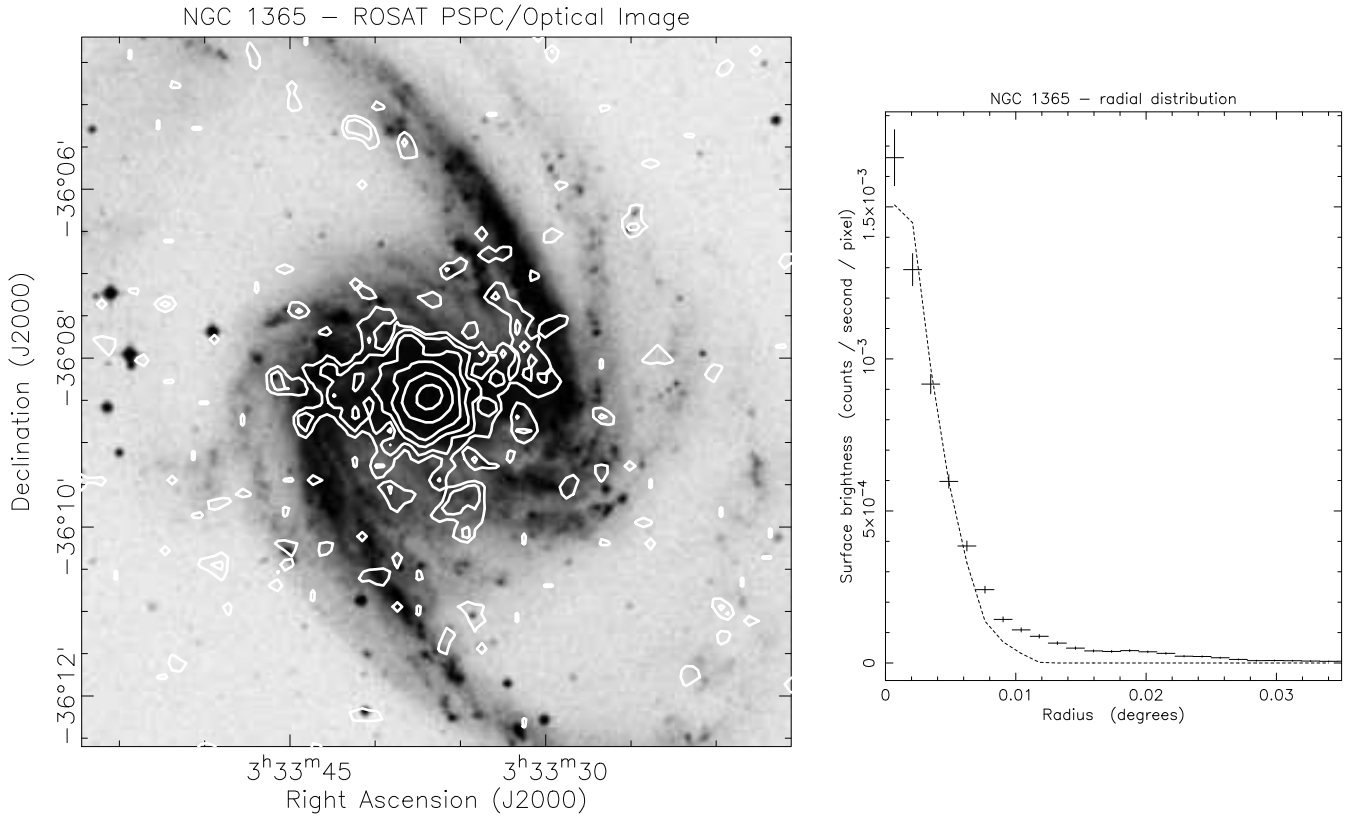


**Figure 2.** Left panel: The X-ray emission from NGC 1365 as seen with the *ROSAT* PSPC. The X-ray contours from the longer PSPC observation are superimposed on the Digitized Sky Survey image of NGC 1365. The lowest contour is at a level of  $5.6 \times 10^{-3}$  cts  $\text{s}^{-1}$  arcmin $^{-2}$ , and increase by a factor 2. Clearly visible is strong X-ray emission from the central region of NGC 1365, as well as extended emission along the galaxy bar, extending out to a radius of about 1.5 arcmin. Several other point sources are also visible and are discussed in Section 4. Right panel: The radial profile of the X-ray emission from the PSPC observations of NGC 1365. Also shown is the PSF for the *ROSAT* PSPC assuming a spectrum with a mean photon energy of 0.7 keV. The X-ray emission is clearly extended, with a radius of about 1.5 arcmin, but also with a point-like central source.

the PSPC, for a spectrum with a mean photon energy of 0.7 keV. The X-ray emission is clearly extended well beyond the PSF of the *ROSAT* PSPC. Also, the extended emission is not azimuthally symmetric, with low surface brightness emission stretching preferentially along the bar of the galaxy. There is also point-like X-ray emission from the central regions of the galaxy. However, as we will discuss later in regard to the HRI observations, this source, which is centred on the optical/radio nucleus, is not point-like, but is extended. Also visible is a point source in the disk of the galaxy to the SW of the nucleus. This source is discussed in more detail in Komossa & Schulz (1998).

In order to investigate the spectral properties of the X-ray emission we have extracted a spectrum from the region within 1.5 arcmin of the central point source for both PSPC observations, and we fit them independently to look for any variability.

We fit both spectra with two different spectral models, i) an absorbed power-law and ii) a single temperature Raymond-Smith plasma model. The details of the fits are given in Table 2. We find that the power-law model gives a poor fit (as was found by Turner *et al.* 1993), with reduced

$\chi^2$  of 1.5 and 2 respectively for the two observations. On the other hand, for the Raymond-Smith plasma models we get good fits (reduced  $\chi^2 \leq 0.7$ ), with  $kT \sim 0.6 - 0.8$  keV, a low metallicity and a column ( $N_H \sim 2 \times 10^{20}$  cm $^{-2}$ ).

The derived luminosities in the *ROSAT* waveband (0.1 – 2.5 keV), corrected for absorption, are  $5 - 6 \times 10^{40}$  erg  $\text{s}^{-1}$ . Adding in an absorbed power-law component to a thermal model (as might be expected if we had a highly absorbed nuclear source) does not lead to a better fit with the PSPC (c.f. Section 2.3).

For the absorbed thermal spectral model, there are some differences in the fitted parameters, mostly notably in the temperature. The differences are only significant at the  $1 - 2\sigma$  level and may not reflect any physical changes.

Komossa & Schulz (1998) also present results from an analysis of the *ROSAT* PSPC observations of NGC 1365. They too note that a single temperature Raymond-Smith model provides a successful fit to the spectra. However, their preferred model is for a two component model, consisting of a Raymond-Smith model plus a powerlaw. The main reasons that Komossa & Schulz (1998) give for preferring the two component model is that the best-fit single temperature

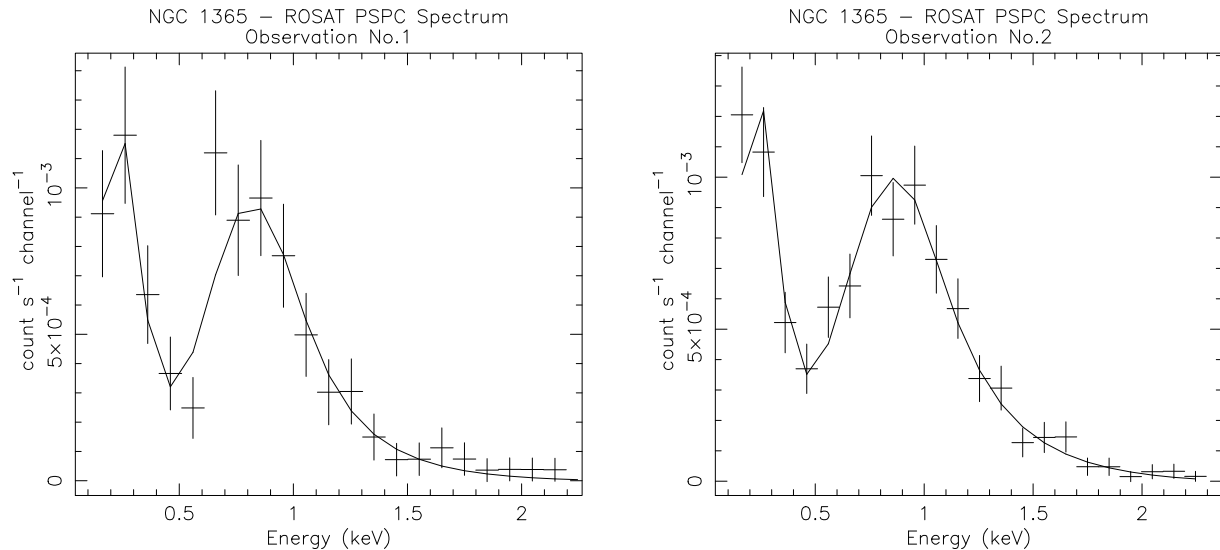


**Figure 3.** The *ROSAT* PSPC spectra of NGC 1365 for both observations. The spectra have been fitted independently and the results are given in Table 2. The model used here is a single temperature Raymond-Smith plasma model.

Raymond-Smith model has a low abundance ( $Z \sim 0.1Z_{\odot}$ ). This low abundance is at odds with optical abundance determinations (Alloin *et al.* 1981) However, we note that the work of Strickland & Stevens (1998) suggests fitting simple (one or two component) spectral models to intrinsically multi-temperature gas (such as would be expected in a starburst) can result in major errors in the fitted metallicity. Consequently, the discrepancy between optical and X-ray determinations should perhaps not be taken too seriously. Komossa & Schulz (1998) also note that a Raymond-Smith plus power-law model is more in line with the *ASCA* results of Iyomoto *et al.* (1997 - see below). On the basis of our spectral fitting of the PSPC spectra we find no statistical reason to prefer a two component model over our single temperature Raymond-Smith model.

It is notable that the X-ray properties of NGC 1365, as observed by the PSPC, are similar, in general terms, to those of starburst galaxies (see Section 4), both in terms of showing extended emission and having an X-ray spectra better fit with a thermal model than a power-law. Also, the fitted column density is very similar to the Stark value ( $N_H = 1.92 \times 10^{20} \text{ cm}^{-2}$ , Stark *et al.* 1992) It is clear that we are not seeing a significant amount of emission in the PSPC waveband from a heavily absorbed Seyfert nucleus, However, the power-law component in such systems (for example, NGC 1386, Iyomoto *et al.* 1997; NGC 7582, Xue *et al.* 1998), associated with the nucleus, has a column  $\geq 10^{23} \text{ cm}^{-2}$ , which means that it will not be detected in the PSPC waveband. We also note that in the case of NGC 1068, a Seyfert 2 galaxy, the power-law component in the X-ray spectrum has a low column (Ueno *et al.* 1994). In NGC 1068 the interpretation is that we are seeing scattered emission from the nucleus, rather than direct emission, the column being too high for it to be directly observed.

We shall discuss the origin of the X-ray emission and the relation to the emission from other Seyfert galaxies in Section 4.

## 2.2 *ROSAT* HRI Observations

There have been two *ROSAT* HRI observations of NGC 1365 (Table 1), of duration 9.8 and 9.9ksec, separated by approximately 18 months. The HRI is less sensitive than the PSPC for diffuse emission but is much better for studying smaller scale spatial structure. The combination of the two instruments allows a detailed analysis of both point source emission and the extended diffuse emission in the central regions of NGC 1365.

The method of analysis that we have adopted for the HRI observations is as follows; we sort a background subtracted image using only channels 3 – 8 to minimise the background (Briel *et al.* 1995). We then search for sources using PSS and adjust the pointing using the position of the BL Lac object 1E 0331.3-3629. The centroids of the X-ray emission from the *ROSAT* HRI and PSPC, as determined by the PSS package, are given in Table 3. We note that the positions of the X-ray centroids only differ from the mean X-ray centroid position by  $\leq 3''$ , and that the mean centroid of the X-ray emission is consistent with the position of the optical/radio nucleus. This point will be discussed in more detail in Section 4.2.

We have generated background subtracted images from both HRI observations. The X-ray/optical morphology as seen with the longer HRI observation is shown in Figure 4. The main features in the X-ray morphology are the central source (which appears to be extended with some evidence of substructure), along with the several other point sources in the disk of the galaxy. Also in Figure 4 we show the radial profile of the central X-ray emission, in conjunction with the PSF for the *ROSAT* HRI. In the PSPC we saw low surface brightness diffuse emission, in conjunction with point-like emission. The HRI gives us an improved picture of the central regions. While there is also low-surface brightness emission seen with the HRI, the central source is now seen to be clearly resolved, with an extent of maybe  $15-20''$ .

**Table 2.** Spectral analysis of *ROSAT* PSPC observations of NGC 1365

Spectral Model (1)	Raymond-Smith spectral model			Power-law spectral model			$L_x$ ( $\text{erg s}^{-1}$ ) (8)
	$N_H$ ( $10^{20} \text{ cm}^{-2}$ ) (2)	$kT$ (keV) (3)	$Z$ ( $Z_\odot$ ) (4)	$N_H$ ( $10^{20} \text{ cm}^{-2}$ ) (5)	$\alpha$ (6)	$\chi^2_\nu$ (7)	
PSPC Observation No. 1							
AG*RS	$1.78^{+0.65}_{-0.65}$	$0.58^{+0.09}_{-0.09}$	$0.074^{+0.05}_{-0.04}$	–	–	0.69 (17)	$5.1 \times 10^{40}$
AG*PL	–	–	–	$5.40^{+1.1}_{-1.1}$	$3.01^{+0.32}_{-0.30}$	1.47 (18)	$2.1 \times 10^{41}$
PSPC Observation No. 2							
AG*RS	$1.91^{+0.45}_{-0.45}$	$0.77^{+0.07}_{-0.06}$	$0.076^{+0.04}_{-0.04}$	–	–	0.69 (18)	$6.2 \times 10^{40}$
AG*PL	–	–	–	$5.64^{+0.07}_{-0.07}$	$2.89^{+0.19}_{-0.18}$	2.09 (19)	$2.3 \times 10^{41}$

Notes on Table2:

Column 1: Spectral model used to fit the data, AG - absorbing component; RS - single temperature Raymond-Smith plasma model; PL - power-law model.

Columns 2-4: Best fit parameters (with errors) for single temperature Raymond-Smith model.

Columns 5-6: Best fit parameters (with errors) for power-law spectral model.

Column 7: Value of the reduced  $\chi^2$  (and number of degrees of freedom in brackets) for the spectral fits.

Column 8: The intrinsic X-ray luminosity (i.e. corrected for absorption). The quoted luminosities for the *ROSAT* PSPC fits are for the 0.1 – 2.5 keV energy band.

Whether this is due to multiple point sources or genuinely diffuse emission is unclear, but its extent is very similar to that of the radio ring (Section 3). Also, in the PSPC observations the emission was extended preferentially along the bar of the galaxy. In the HRI observations we are sampling emission from a smaller, more central region, and in contrast to the PSPC observations there is no evidence of significant azimuthal variation in the HRI observations.

The point source searching program PSS detected several other point sources in close vicinity to the nucleus. In addition to genuine point sources we may also be detecting peaks in the more extended emission seen in the PSPC. The fact that we definitely see extended X-ray emission from the central regions with the HRI strongly suggests that we are genuinely seeing diffuse emission.

### 2.3 ASCA Observations

Because of its wider waveband (0.5 – 10.0 keV) and higher spectral resolution, *ASCA* observations of NGC 1365 can potentially tell us more about the origin of the X-ray emission from the central source - in particular, whether there is a highly absorbed power-law component, as is seen in some other Seyfert 2 galaxies.

On account of the poor spatial resolution of *ASCA* (typically  $\sim 3'$ ), and the presence of the source in the disk of the galaxy there is likely to be a problem of contamination in the spectra of the central source.

Results from *ASCA* observations of NGC 1365 have already been reported on in some detail in Iyomoto *et al.* (1997). Rather than repeat the analysis we shall quote the main results from this paper, which can be summarised as follows:

- (i) A hard point-like source was detected at a position coincident with the centre of NGC 1365.
- (ii) The continuum spectra could be fitted with a power-law (with a photon index of  $\sim 0.8$ ) plus a Raymond-Smith

plasma model (with a  $kT = 0.85$  keV and a metallicity of  $0.2Z_\odot$ ). At energies  $< 2$  keV the thermal component dominates over the power-law.

(iii) The power-law component did not require substantial excess absorption.

(iv) The 2 – 10 keV luminosity of the power-law component was found to be  $4 \times 10^{40} \text{ erg s}^{-1}$  (for an assumed distance of 20 Mpc).

(v) Also present in the spectrum was a strong, broad Fe-K line, with a line centre energy of 6.6 keV and a width of 0.2 keV.

These results are very important for a number of different reasons. First, the detection of strong Fe-K emission from a galaxy is usually an indicator of an active nucleus, although the luminosity of the power-law component in NGC 1365 is rather low compared to the power-law components in other Seyfert galaxies. A second important point is that the power-law component is not highly absorbed. This is similar to NGC 1068 (Ueno *et al.* 1994), but dissimilar to several other Seyfert 2 galaxies, where in addition to a thermal component a hard *highly absorbed* power-law component is seen (examples include NGC 1386, Iyomoto *et al.* 1997; NGC 4388, Iwasawa *et al.* 1997; NGC 7582, Xue *et al.* 1998).

The metallicity for the Raymond-Smith component of the fit to the *ASCA* data ( $0.2Z_\odot$ ) is somewhat higher than the metallicity determined from the PSPC results. However, given the respective error-bars the results are not inconsistent (see also Strickland & Stevens 1998).

We shall discuss the implications of the *ASCA* results at length in Section 4.

### 3 RADIO OBSERVATIONS OF NGC 1365

Radio continuum observations of NGC 1365 using the ATCA have been presented by Forbes & Norris (1998). Radio maps

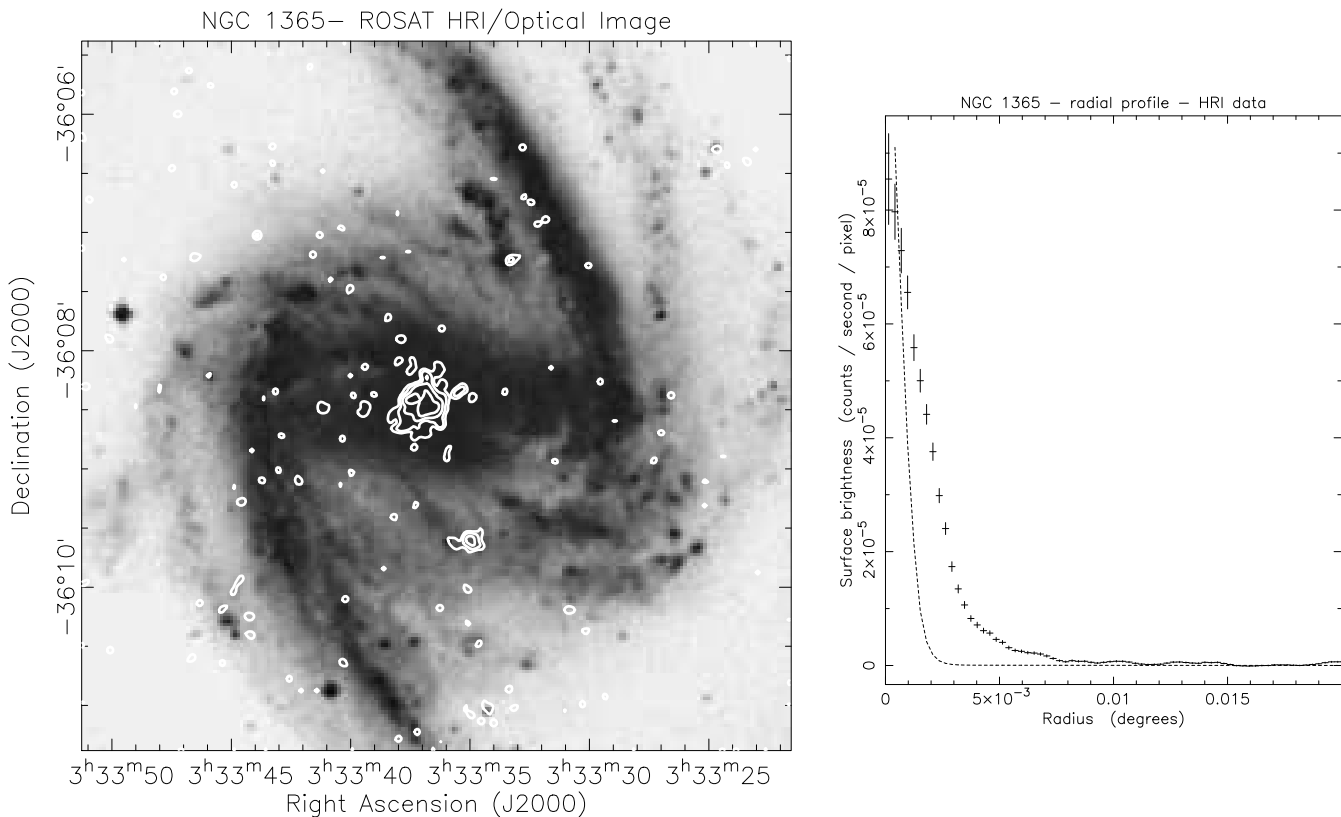


**Figure 4.** Left panel: The X-ray emission from NGC 1365 as seen with the ROSAT HRI. The X-ray contours are from the longer HRI observation and are superimposed on an optical image from the Digitized Sky Survey image. The X-ray image has been background subtracted, and has been extracted with a  $1''$  pixel size and smoothed with a Gaussian of FWHM  $3''$ . The lowest contour level is at a level of  $2.2 \times 10^{-2}$  cts  $s^{-1}$  arcmin $^{-2}$  and the contours increase by a factor 2. There is strong X-ray emission from the central point source, as well as several point sources near to the nuclear source. The BL Lac object used to register the image is not shown. The point source to the SW of the nucleus is probably associated with an HII region visible in this image. The spatial resolution of the ROSAT HRI is  $\sim 5''$ . Right panel: The radial profile of the central point source compared to the ROSAT HRI PSF. The central source is clearly extended.

**Table 3.** The centroids of the X-ray emission from the central source in NGC 1365 as compared to the positions of the optical and radio position of the nucleus (Alloin *et al.* 1981; Forbes & Norris 1998)

Observation	RA (J2000)	Dec
PSPC Obs. 1	03 33 36.5	-36 08 25
PSPC Obs. 2	03 33 36.4	-36 08 27
HRI Obs. 1	03 33 36.4	-36 08 28
HRI Obs. 2	03 33 36.4	-36 08 25
Average	03 33 36.4	-36 08 26.3
Optical Position	03 33 36.4	-36 08 25.7
Radio Position	03 33 36.35	-36 08 25.9

were obtained at 3cm and 6cm giving an effective resolution of  $\sim 1''$  and  $\sim 2''$  respectively. Forbes & Norris (1998) examined the overall radio properties of NGC 1365 along with five other southern active galaxies. They did not discuss the

individual hotspots in any detail. In Figure 5 we show only the 3cm radio maps of the central regions.

The radio maps reveal a weak nucleus surrounded by a elongated  $\sim 8'' \times 20''$  ( $a/b = 0.4$ ) ring of hotspots. Sandqvist *et al.* (1995) labelled the hotspots A–H, although B is blended with A, and C is blended with D at our  $1''$  resolution. Forbes & Norris (1998) identified an additional hotspot to the SW, called ‘J’. Components E, H and J are marginally resolved in our 3cm map, so that typical component sizes are  $\sim 1''$  or 100 pc at our assumed distance of 20 Mpc. Centering on the component flux peak, we have measured positions and  $2''$  diameter fluxes. We have chosen to subtract the background in an annulus around each component rather than subtract a constant background as done by Sandqvist *et al.* (1995). Thus we do not expect very close agreement between our measurements (given in Table 4) and those of Sandqvist *et al.* (1995). However we might expect our 6/3 cm spectral index to be similar to their 6/2 cm index. For the nucleus itself Sandqvist *et al.* (1995) find  $\alpha < -0.87$  for 6/2 cm, which is consistent with our value of  $\alpha = -1.1$  for 6/3 cm. For components A, D and F, we get comparable

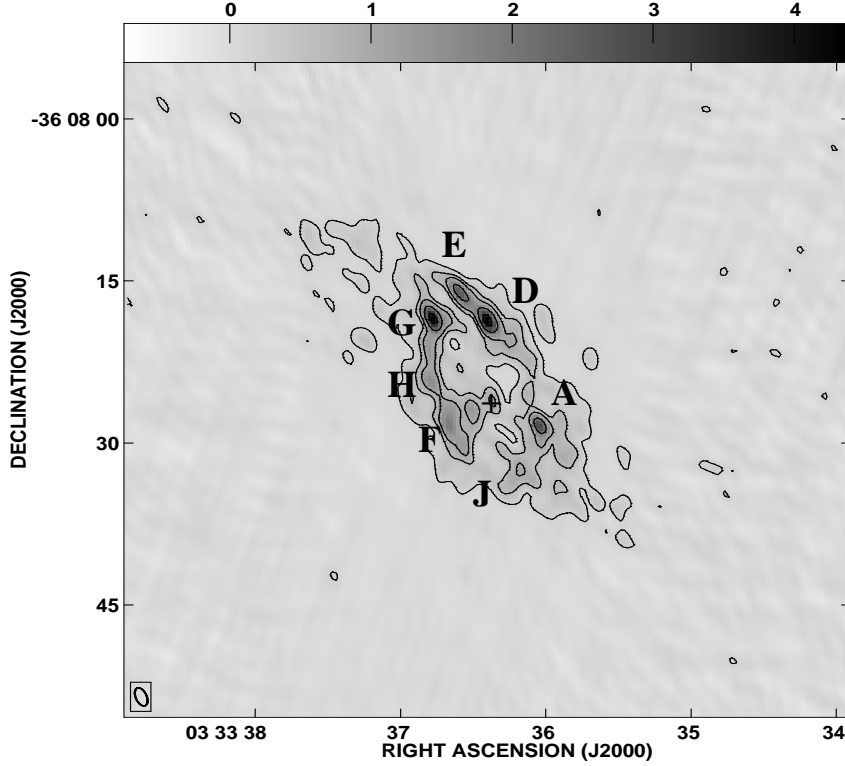


**Figure 5.** The 3cm ATCA radio map of the central region of NGC 1365. A number of hotspots in an elongated ring structure surrounding a weak nucleus can be seen, and are labelled as in Table 4. The position of the nucleus is marked with a cross. The beam size ( $\sim 1''$ ) is shown in the lower left. The upper greyscale bar shows the intensity scale in mJy/beam.

indices. In the case of component E and G, their values (ie  $\alpha = -0.77$  and  $-0.44$  respectively) are considerably different from ours ( $\alpha = -0.4$  and  $-0.04$ ). Most of the components in the ring have moderate to steep spectral indices which are consistent with non-thermal emission. The typical hotspot 6cm luminosity is  $10^{36}$  erg  $s^{-1}$  which, along with the steep spectral index, suggests that the radio emission from each hotspot is made up of several SNRs.

Sandqvist *et al.* (1995) have suggested that component F represents the end of a “jet-like feature” emanating from the nucleus. They found component F to have the steepest spectral index, other than the nucleus. Our data indicate that both component H and J have similarly steep indices. An alternative explanation to the radio jet is that of a nuclear bar which extends out to the radio ring. Enhanced star formation is often seen at the ends of a bar in barred galaxies. The nature of the nucleus in NGC 1365 is difficult to confirm with our radio data. It is unresolved in the 3cm map. The steep spectral index indicates non-thermal synchrotron from either an AGN or SNRs. We note that energetically a small number of Cas A-like SNRs can account for the radio emission.

#### 4 DISCUSSION

The main points that can be distilled from these observations are as follows:

(i) The *ROSAT* PSPC observations show extended X-ray emission from the central region of NGC 1365, with the emission preferentially extended along the bar of the galaxy. The

**Table 4.** NGC 1365 Radio Hotspots

Hotspot	Position (s, ")	6cm flux (mJy)	3cm flux (mJy)	Sp. Index
Nuc.	36.35, 25.9	0.46	0.24	-1.1
A	36.02, 28.3	1.25	0.97	-0.4
D	36.37, 18.6	2.11	1.47	-0.6
E	36.57, 16.0	1.01	0.80	-0.4
F	36.63, 28.0	1.06	0.63	-1.0
G	36.75, 18.3	1.60	1.56	-0.04
H	36.76, 24.1	1.00	0.58	-1.0
J	36.15, 32.8	0.65	0.37	-1.0

Notes to Table 4.

Galaxy nucleus at  $03^h33^m36.35^s$ ,  $-36^\circ08'25.9''$  (J2000).

PSPC spectra can be well fitted with a thermal model with  $kT \sim 0.6-0.8$  keV and a low absorbing column, comparable to the Galactic Stark value.

(ii) The *ROSAT* HRI observations show that the more concentrated central X-ray emission is still extended, with a radius of  $\sim 15''$  (1.5 kpc), similar in extent to the radio ring.

(iii) The centroid of the X-ray emission is consistent with the position of the radio/optical nucleus (see Section 4.2).

(iv) The *ASCA* observations suggest that, in addition to the softer thermal emission, there is also a power-law component which is not highly absorbed.

(v) The *ASCA* results also show strong Fe-K emission, indicative of an active nucleus.

(vi) The radio observations reveal a steep spectrum but the radio emission from the nucleus is less than that of

the surrounding hotspots. The evidence for a radio jet is marginal.

#### 4.1 Broad-band properties

Having estimated the total X-ray emission from NGC 1365 (i.e.  $L_x \sim 6 \times 10^{40}$  erg s<sup>-1</sup> in the 0.1–2.5 keV energy band) we can compare its X-ray properties to those of other spiral, starburst and Seyfert galaxies. Its total blue luminosity is  $L_B = 4.6 \times 10^{10} L_\odot$  and the IRAS far-infrared flux between 40  $\mu$ m and 120  $\mu$ m, using the expression in Helou *et al.* (1988), gives a luminosity of  $L_{FIR} = 6.8 \times 10^{10} L_\odot$ . Assuming the conversion of Hunter *et al.* (1986) this corresponds to a star formation rate for stars with masses  $\geq 0.1 M_\odot$  of about  $18 M_\odot \text{ yr}^{-1}$ .

From the relationship between  $L_x$  and  $L_{FIR}$  for starburst galaxies in David, Jones & Forman (1992), and using the FIR luminosity of NGC 1365 we can estimate the fraction of the X-ray luminosity that we might expect from the starburst component. On this basis, the David *et al.* (1992) relationship would predict a soft X-ray luminosity of  $\sim 10^{41}$  erg s<sup>-1</sup>, comparable to the luminosity in the ROSAT PSPC waveband (Table 2, see also Turner *et al.* 1997). We can also compare the values of  $L_x$ ,  $L_B$  and  $L_{FIR}$  for NGC 1365 with those for the sample of nearby spirals and starburst galaxies in Read, Ponman & Strickland (1997). We find that NGC 1365 lies roughly on the  $L_x : L_B$  correlation found by Read *et al.* (1997), though NGC 1365 is more X-ray luminous than any galaxy in the sample of Read *et al.* (1997). These facts suggest that the bulk of the soft X-ray emission is due to starburst activity.

An interesting comparison can also be made between the properties of NGC 1365 and those of WR galaxies in the survey of Stevens & Strickland (1998). WR galaxies are believed to be young starbursts, and we note that NGC 1365 can be regarded as a WR galaxy on account of the WR feature in one of the HII regions in the central regions (region L4). However, it is unlike many of the other WR galaxies in the sample of Stevens & Strickland (1998), which often are dwarf galaxies. Contini *et al.* (1995) included NGC 1365 in their sample of barred spiral WR galaxies - all of which seem to have a high inclination. Contini *et al.* (1995) suggested that starburst winds may play a role in removing absorbing material perpendicular to the galaxy disk, making the WR feature more likely to be observed. The X-ray spectra from the nuclear regions of NGC 1365 shows very little local absorption, which may provide some support for this idea. In terms of the  $L_x : L_B$  relationship, NGC 1365 lies rather below the trend for WR galaxies found by Stevens & Strickland (1998). However, the spectrum of NGC 1365 is very similar to those of WR galaxies. The fact that NGC 1365 is also a WR galaxy strengthens the contention that the soft X-ray emission from NGC 1365 is mostly due to starburst emission.

The relationship between radio and far-infrared luminosity extends over many orders of magnitude and includes normal spirals, starburst galaxies and radio-quiet Seyfert galaxies (e.g. Wunderlich, Wielebinski & Klein 1987). In the case of NGC 1365 the far-infrared to radio lies between the typical values for normal and starburst galaxies (Helou *et al.* 1985) further indicating that the bulk of the far-infrared

and radio emission is associated with star formation processes rather than any AGN.

The Brackett  $\gamma$  emission has been used as a predictor of X-ray emission from starbursts (Ward 1988). In this model all of the predicted X-ray emission from the starburst comes from massive X-ray binaries (MXRBs), which are formed from the binary evolution of massive stars. The Brackett  $\gamma$  emission is a consequence of recombination following ionization by the same set of massive stars formed in the starburst. The predicted relationship between  $L_x$  (for soft X-rays) and  $L_{B\gamma}$  is:

$$L_x(\text{erg s}^{-1}) = 7 \times 10^{-35} \frac{L_{B\gamma} L_{MXRB}}{R} \quad (1)$$

where  $L_{MXRB}$  is the mean X-ray luminosity per massive X-ray binary (which we assume to be  $10^{38}$  erg s<sup>-1</sup>) and  $R$  is the number of MXRBs per O-star. We assume  $R = 500$  (Fabbiano *et al.* 1982). This relationship clearly does not take into account X-ray emission from superbubbles or SNRs or an AGN.

From Forbes & Ward (1993) we calculate that the Brackett  $\gamma$  luminosity in the central 6'' is  $L_{B\gamma} = 1.44 \times 10^{39}$  erg s<sup>-1</sup>, which in turn implies a total number of O-stars of around  $10^5$ , and an  $L_x = 2 \times 10^{40}$  erg s<sup>-1</sup>. This is only a factor of 3 or so below our preferred thermal model estimate for  $L_x$  of the whole galaxy, suggesting that the contribution of an AGN to the low energy X-ray emission from NGC 1365 may be small. The main caveat here is that MXRBs in our own Galaxy have much harder spectra (typically a powerlaw with a high energy cut-off - Nagase 1989) than that observed from NGC 1365. It is possible that the power-law in the ASCA observations could be a consequence of these MXRBs. However, the line emission could not be generated by a population of MXRBs.

#### 4.2 The Location of the X-ray Nucleus

As noted earlier we can use the optical position of the BL Lac object 1E 0331.3-3629 to register the X-ray images, which in turns enables us to determine the centroids of the X-ray emission from the central regions of NGC 1365.

In Table 3 we list the positions of the centroids of the X-ray central source as determined by the PSS program, for all the ROSAT observations. There is some scatter between the X-ray determined positions, but this is  $\leq 2''$ , indicating good consistency between the results for the different ROSAT observations. The positions of the radio and optical nucleus are also listed in Table 3.

The mean centroid of the X-ray emission is consistent with the position of the optical/radio nucleus. This might suggest that we are seeing emission from a massive compact object in the nucleus. There are several arguments against this; first, the HRI observations (Fig. 4) show that the central X-ray emission is extended and not point-like, with an extent comparable to the radio ring (and the X-ray emission is also centred on the radio ring). Second, the X-ray spectral properties as seen with ROSAT, are consistent with thermal radiation, but not with power-law emission expected from a compact object, although as the ASCA results of Iyomoto *et al.* (1997) show there is emission at higher energies from an active nucleus. Also, a peak in the X-ray emission peaks

coincident with the position of the optical/radio nucleus is seen in other nuclear starbursts (c.f. Ptak *et al.* 1998).

Consequently, the X-ray emission is centred on the nucleus of the galaxy. This does not mean that the X-ray emission is dominated by a central point source, as the *ROSAT* observations suggest that at soft X-ray energies the emission is dominated by a nuclear starburst. While there appears to be emission associated with an active nucleus at higher energies its contribution at soft X-ray energies is small compared to the hot thermal emission. *AXAF*, with its  $\sim 0.5''$  spatial resolution, will provide a much clearer view of the complex morphology in the heart of NGC 1365.

#### 4.3 Origin of the Radio Emission

The spectral indices of the radio hotspots imply a non-thermal origin. The spatial morphology - a ring around the nucleus - tells us that a compact object is not responsible for the vast majority of the radio emission. Supernovae or SNRs are the obvious candidates for the hotspot emission with synchrotron emission from shock accelerated electrons the most likely emission mechanism.

If the typical radio luminosity of a SNR is  $L_{6cm} \sim 10^{33} \text{ erg s}^{-1}$  and in the central  $6''$  of NGC 1365 we have  $L_{6cm} = 2.3 \times 10^{37} \text{ erg s}^{-1}$ , this would imply 23,000 SNRs. However, the emission from young radio supernovae can be much more luminous than this (i.e. SN1988Z; van Dyk *et al.* 1993), and these ‘radio supernovae’ could be responsible for much of the emission from one or other of the radio hotspots. Further to this, some ‘radio supernovae’ have also been detected as bright X-ray sources (for instance, Fabian & Terlevich (1996) found that SN1988Z has an X-ray luminosity in the *ROSAT* waveband of  $L_x \sim 10^{41} \text{ erg s}^{-1}$ , brighter or comparable in luminosity to many starburst galaxies). Indeed we can correlate the positions of the HII regions near the centre of NGC 1365 (Alloin *et al.* 1981) with the radio hotspots. The HII region L3 and radio hotspot A seem to be connected, as do L12 and hotspot E. Kristen *et al.* (1997), reporting on *HST* observations of NGC 1365, find a positional coincidence between a super star cluster and radio hotspot A. On this basis, and the probable strong  $H\alpha$  emission from this cluster, suggest that the radio emission from hotspot A is due to a radio supernova.

It is instructive to compare  $L_x/L_{6cm}$  ratios for different objects. Sgr A\*, the black hole at the centre of our Galaxy, has a soft X-ray luminosity of  $L_x \sim 10^{34} \text{ erg s}^{-1}$  (Predehl & Trümper 1994) and a 6cm luminosity of  $L_{6cm} \sim 10^{33} \text{ erg s}^{-1}$  (Marcaide *et al.* 1992) for an assumed distance of 8.5 kpc. So the  $L_x/L_{6cm}$  ratio is 10. Cas A, the brightest SNR in our Galaxy, has an  $L_x/L_{6cm}$  ratio of  $\sim 75$ . For radio supernovae the ratio can be higher still ( $L_x/L_{6cm} \sim$  several hundred) for SN1988Z and SN1978K.

Because of the complex extended nature of the emission, and the limitations of the X-ray instruments it is a difficult to accurately estimate the X-ray flux from within  $6''$ . We estimate a value of  $\sim 1 - 2 \times 10^{40} \text{ erg s}^{-1}$ . For NGC 1365 we have  $L_{6cm} = 2.3 \times 10^{37} \text{ erg s}^{-1}$ , which implies a ratio of  $L_x/L_{6cm} \sim 400 - 1000$  within a radius of  $6''$ . This value is rather large and could suggest that an AGN is not the dominant energetic factor in the central regions of NGC 1365, and is more in line with that seen for radio supernovae. Of relevance is the fact that the  $L_x/L_{6cm}$  ratio for NGC 1068

is also in the range 500 – 1000 (see Condon *et al.* 1982 for larger aperture radio observations of NGC 1068). For both NGC 1365 and NGC 1068 the emission from the nucleus (as identified at higher resolution) is much less than the emission from within a radio of  $6''$  (see Table 4 and Muxlow *et al.* 1996). We also note that large values of  $L_x/L_{6cm}$  are possible in radio quiet QSOs (c.f. Mas-Hesse *et al.* 1995).

#### 4.4 Origin of the Extended X-ray emission

There are perhaps three main possible explanations for the extended X-ray emission seen in NGC 1365; first, scattering of nuclear radiation by photoionized material, second, a large number of unresolved point sources, and third, genuinely extended X-ray emission from a hot plasma.

##### 4.4.1 Scattering of Nuclear Emission

Extended X-ray emission has also been found in the Seyfert 2 galaxy NGC 4388 by Matt *et al.* (1994), using results from the *ROSAT* HRI. Results from PSPC observations of NGC 4388 have been reported on in Antonelli, Matt & Piro (1997). These authors discussed the possibility that a luminous nuclear source (i.e. a supermassive black-hole) photoionizes a large region around it, but is obscured from direct view by a dense torus. Radiation escaping perpendicular to the torus is scattered into the line-of-sight by electrons from the photoionized plasma. Matt *et al.* (1994) discounted this idea largely on the basis of the observed spectral properties of NGC 4388.

In NGC 1365, the *ASCA* observations suggest the presence of a scattered component, which might well be associated with a luminous nucleus obscured from direct view. This scattered power-law component cannot be responsible for the bulk of the soft emission seen in the *ROSAT* waveband for the following reasons. First, the X-ray emission as seen by the *ROSAT* PSPC is very extended (8 kpc), which would imply an extremely luminous ionizing source, and second, and perhaps most telling, is that the observed thermal spectrum, is too soft to result from the scattering of a AGN continuum.

##### 4.4.2 Unresolved Point Sources

Populations of stellar sources distributed throughout the bar of NGC 1365 could mimic the extended nature of the emission by such an ensemble. These objects could be X-ray binaries (both high and low mass), normal stars (again both high or low mass) or supernova remnants.

Both high mass and low mass X-ray binaries have harder spectra than the  $\sim 0.7 \text{ keV}$  thermal spectrum observed in NGC 1365. The X-ray luminosity of NGC 1365 is rather high for a typical spiral (but not excessively so). A model whereby a reasonably large number of MXRBs were emitting could be plausible. We note that MXRBs are descendants of high mass stars and will be formed in starburst events, and so this model is not completely distinct from models associated with starbursts.

As noted in Section 4.1, the Brackett  $\gamma$  emission can be used to estimate the number of O-stars and X-ray binaries. For NGC 1365 the number of X-ray binaries is of order 200.

If these 200 binaries were uniformly distributed in a disk of radius 8 kpc then the mean separation would be significantly below that of the *ROSAT* PSPC but comparable to that of the HRI. We see from both PSPC and HRI observations that the emission from the extended component is clearly concentrated towards the central region. Consequently such a model with  $\sim 200$  luminous MXRBs distributed through the bar of the galaxy could account for the spatial properties seen in NGC 1365. As we have noted before the X-ray spectral properties would suggest that MXRBs were not the dominant source of emission.

An origin associated with early-type stars can be quickly dismissed - these typically have  $L_x/L_{bol} \sim 10^{-7}$ , implying too low a level of X-ray emission. While magnetically active low-mass stars can have higher  $L_x/L_{bol}$ , such a large population of young active stars would be implausible.

Individual SNR can have X-ray luminosities of  $L_x \sim 10^{34} - 10^{36} \text{ erg s}^{-1}$ , and X-ray temperatures of the right magnitude (Schlegel 1995). Young ( $\leq 20 \text{ yr}$ ) ‘radio supernovae’ can have X-ray luminosities higher luminosities ( $10^{39} \text{ erg s}^{-1}$  or more), but these luminosities are short lived. A situation where we have a large number of SNR ( $10^5 - 10^6$ ) could give rise to observed the X-ray luminosity. However, for any reasonable estimate of time-scale for substantial X-ray emission to persist from an individual SNRs (a few  $10^3$  years) this would imply a very high SN rate, at odds with observations at other wavelengths. The SN rate in the central  $6''$ , as inferred from the radio observations, is 0.02 SN/yr, and 0.03 SN/yr, as inferred from [FeII] emission (Forbes & Norris 1998).

We can probably rule out a SNR origin for all of the X-ray emission by reference to the radio observations, which imply a much smaller number of SNRs. However, as we shall discuss below, a starburst origin of the X-ray emission would still imply a contribution from supernovae, but in this case the hot gas from a starburst will have been built up over a long period of time.

We note that there have been two historical supernova in NGC 1365; SN1957C, to the N of the nucleus and the type Ic SN1983V, about 1 arcmin to the SW of the nucleus (Clocchiatti *et al.* 1997). Neither SN are coincident with any X-ray or radio source.

#### 4.4.3 Extended hot gas

The most plausible physical origin for extended hot gas in the disk of NGC 1365 is from a starburst. Here a burst of star-formation results in the production of large numbers of massive OB stars, which via their stellar winds and subsequent supernova inflate X-ray emitting superbubbles, which will eventually merge and blow-out to form a superwind, such as seen in M82 (Strickland, Ponman & Stevens 1997, Moran & Lehnert 1997).

The simple analysis concerning the Brackett  $\gamma$  emission suggests the presence of around  $10^5$  O9 stars (or their equivalent). The mass-loss rate of such a star is  $\sim 10^{-6} M_\odot \text{ yr}^{-1}$  and the wind kinetic energy is of order  $10^{36} \text{ erg s}^{-1}$ , so the total kinetic energy from such a cluster of stars (assuming they are all concentrated towards the centre of the galaxy) will be  $10^{41} \text{ erg s}^{-1}$ . As only a fraction of the kinetic energy of the stellar winds can be converted into X-ray emission such an assembly of stars would not, by themselves, be able

to power the X-ray emission from NGC 1365. However, this analysis does not account for the contribution from SNRs and X-ray binaries, and the hot stars could make a significant contribution to the X-ray emission via their stellar winds.

#### 4.5 Comparison with other Seyfert 2 galaxies

In order to understand the radio/X-ray properties of NGC 1365 we now briefly discuss similar observations of related galaxies.

Turner *et al.* (1993), in addition to presenting results on NGC 1365, also presented *ROSAT* PSPC results on several Seyfert 2 galaxies. Of note is that it was not possible to obtain a good fit with a power-law model for NGC 1365, while much better fits were obtained for the other galaxies in the sample. Also, the other galaxies were typically an order of magnitude more X-ray luminous than NGC 1365, and were much more overluminous compared to their blue luminosity. This would suggest that NGC 1365 is not a typical Seyfert 2, but as we shall see in the discussion below, there are some striking similarities between the X-ray properties of NGC 1365 and some other galaxies classified as Seyfert 2’s.

Awaki (1997) reviews the X-ray properties of Seyfert 2s, finding an extremely wide range of luminosities, with some galaxies having luminosities of  $5 \times 10^{43} \text{ erg s}^{-1}$ , while others have  $L_x \sim 10^{41} \text{ erg s}^{-1}$ . The radio emission from Seyfert 2s may cover an even larger range of 4 – 5 orders of magnitude (see for example Simpson *et al.* 1996).

Wilson *et al.* (1992) have reported on *ROSAT* HRI observations of the canonical Seyfert 2 galaxy NGC 1068. These observations revealed a compact nuclear source, circumnuclear emission (with a diameter of 1.5 kpc) and much more extended emission (diameter 13 kpc) associated with the starburst disk. Wilson *et al.* (1992) concluded that the nuclear and circumnuclear X-ray emission were from thermal gas associated with an outflowing wind.

Higher spectral resolution X-ray observations of NGC 1068 with both *BBXRT* and *ASCA* (Marshall *et al.* 1993; Ueno *et al.* 1994) found strong line emission from a range of different species, including strong Fe-K emission. In addition, the X-ray continuum could be fitted with a model with two soft thermal components (with one component with  $kT < 0.2 \text{ keV}$  and a 2nd component with  $kT \sim 0.4 - 0.7 \text{ keV}$ ) and a power-law component, with a photon index of  $\sim 1.3$ . Importantly, the power-law component does not appear to be highly absorbed. According to Marshall *et al.* (1993) the 2-10 keV luminosity of NGC 1068 (dominated by the power-law component) is  $\sim 2 \times 10^{41} \text{ erg s}^{-1}$ , approximately an order of magnitude brighter than the powerlaw component for NGC 1365 (Iyomoto *et al.* 1997).

Marshall *et al.* (1993) and Ueno *et al.* (1994) developed a model for NGC 1068 whereby the X-ray emission is due to both starburst emission and scattered emission from a much more luminous (possibly  $10^{43} \text{ erg s}^{-1}$ ) active nucleus. In this picture we see no direct X-ray emission from the active nucleus (it being obscured by material with an extremely high column), only emission scattered into the line of sight by both warm and hot absorbing material.

It is worth noting that at radio wavelengths the nucleus of NGC 1068 is much brighter than NGC 1365 (Muxlow *et al.* 1996). The source that Muxlow *et al.* (1996) identify

with the nucleus of NGC 1068 in addition to having an inverted spectrum, is well over an order of magnitude brighter than the source identified with the nucleus in NGC 1365. With larger apertures NGC 1068 is still much brighter at radio wavelengths than NGC 1365 (c.f. Section 4.3; Condon *et al.* 1982). On spatial scales of several arcseconds the radio emission is dominated by starburst/SNR emission, with only a small contribution from the nucleus.

Matt *et al.* (1994) have reported on *ROSAT* HRI observations of NGC 4388, a highly inclined spiral galaxy (SB(s)b pec) near the core of the Virgo cluster, finding extended emission with a radius of 4.5 kpc. Matt *et al.* (1994) did not find any evidence of a central source, constraining the emission from such a point source to less than 20% of the total.

NGC 4388 also shows weak broad H $\alpha$  emission in extended off nuclear regions (Shields & Filippenko 1988), which has been interpreted as being due to scattered light from an obscured nucleus (as per the standard unified model of Seyfert 2 nuclei). NGC 4388 also has two extended and asymmetric ionization cones. Iwasawa *et al.* (1997) have also studied the X-ray properties of NGC 4388 including *ASCA* observations. The *ASCA* observations reveal the presence of a strong and highly absorbed ( $N_H = 4 \times 10^{23} \text{ cm}^{-2}$ ) power-law component coming from the nucleus, along with narrow Fe line emission at 6.4 keV (though this emission line has a large equivalent width (EW  $\sim 500 \text{ eV}$  - Iwasawa *et al.* 1997).

Brandt, Halpern & Iwasawa (1996) have reported on *ROSAT* PSPC and HRI observations of the composite starburst/Seyfert 2 NGC 1672 (SB(s)b). Of three X-ray sources associated with NGC 1672, the nuclear source (X-1) has an unabsorbed luminosity of  $L_x \sim 10^{40} \text{ erg s}^{-1}$  in the *ROSAT* waveband,  $kT = 0.7 \text{ keV}$  and a low absorbing column ( $N_H = 1.6 \times 10^{20} \text{ cm}^{-2}$ ). The X-ray luminosity of NGC 1672 is somewhat lower than for NGC 1365, but otherwise the X-ray properties are remarkably comparable. NGC 1672 also shows a compact radio source located at the optical nucleus, with an almost circular ring of emission, as seen in NGC 1365 (Sandqvist *et al.* 1995). Consequently, NGC 1672 may indeed be very similar to NGC 1365, and the Seyfert nucleus may also not play a dominant role in this galaxy.

#### 4.6 Is there a Seyfert Nucleus in NGC 1365 ?

As noted in the introduction, NGC 1365 has been classified as a galaxy with a Seyfert nucleus on the basis of both broad and narrow H $\alpha$  emission. On the basis of the *ROSAT* data there is no real evidence at soft X-ray energies of a Seyfert type nucleus in NGC 1365. However, the *ASCA* data does suggest the presence of an active nucleus. We suggest that the active nucleus in NGC 1365 is a low-luminosity analogue of that in NGC 1068, with a luminosity of 5-10% of that in NGC 1068. So that, while in NGC 1068 it has been suggested that the AGN perhaps provides approximately 50% of the bolometric luminosity (Telesco *et al.* 1984). We suggest that in NGC 1365 the fraction provided by the AGN will be correspondingly smaller.

There is also evidence of something resembling an active nucleus at radio wavelengths, but whether it is strong enough to warrant NGC 1365 being classified as a Seyfert nucleus is questionable. At optical wavelengths, there is some evidence of AGN related activity - with an outflow cone seen in [OIII]  $\lambda 5007$ , though an outflow like this could be gener-

ated by starburst activity. As to the broad H $\alpha$  emission - could the radio supernova associated with radio hotspot A be responsible for this?

Recently, when discussing massive black holes in galaxies it has become popular to suggest that many black holes are not accreting at the Eddington rate but rather the much reduced rate associated with an advection dominated accretion flow (ADAF; Narayan 1996). We consider the presence of an ADAF in NGC 1365 to be unlikely, on the basis of both the radio and X-ray spectra. Such ADAFs predict a slightly positive spectral index at radio wavelengths. We find that the 6/3 cm index is quite steep at  $-1.1$ , and we do not see much evidence for a very hot bremsstrahlung spectrum from the nucleus (though this component could possibly be mistaken for the observed power-law component), though its absence would have to be confirmed by *AXAF*. An unobscured ADAF would also not produce strong Fe-K line emission (Narayan 1996).

NGC 1365 is a highly inclined system, with  $i \sim 60^\circ$ , so that, in a more speculative vein, we could be looking down onto a superwind, such as seen in M82. Neither the X-ray temperature nor luminosity are unreasonable for such a model, and this idea merits further investigation. As mentioned earlier, an outflow cone has been observed in this galaxy, though it was thought to be related more to AGN activity.

In summary, we have presented radio and X-ray observations of the prominent barred spiral NGC 1365. On the basis of soft X-ray and radio observations we find little if any evidence of an AGN, but much more evidence for strong star-forming activity. However, strong Fe-K emission does suggest an active nucleus. Comparison with other Seyfert galaxies, such as NGC 1068, suggest that any AGN in NGC 1365 is not energetically dominant at most wavelengths. Consequently, we suggest that the active nucleus in NGC 1365 is a low luminosity analogue of the nucleus in NGC 1068. Even in the nucleus of NGC 1365, AGN activity is accompanied by very significant starburst emission, and outside of the nuclear region starburst activity completely dominates.

#### ACKNOWLEDGEMENTS

The anonymous referee is thanked for a very helpful report which significantly improved the quality of the paper.

IRS acknowledges funding from PPARC. The data analysis presented in this paper made use of the *STARLINK* node at the University of Birmingham, and the *ASTERIX* package. This research has made use of data obtained from the Leicester Database and Archive Service at the Department of Physics and Astronomy, Leicester University, UK. The Digitised Sky Surveys were produced at the Space Telescope Science Institute under U.S. Government grant NAG W-2166. The images of these surveys are based on photographic data obtained using the Oschin Schmidt Telescope on Palomar Mountain and the UK Schmidt Telescope.

#### REFERENCES

Allan D. J., 1993, *ASTERIX* User Note No. 4.

- Alloin D., Edmunds M. G., Lindblad P. O., Pagel B. E. J., 1981, *A&A*, 101, 377
- Antonelli L. A., Matt G., Piro L., 1997, *A&A*, 317, 686
- Awaki H., Ueno S., Koyama K., Iwasawa K., Kunieda H., 1997, *Adv. Sp. Res.*, 19, 95
- Brandt W. N., Halpern J. P., Iwasawa K., 1996, *MNRAS*, 281, 687
- Briel U. G., *et al.* 1995, "The *ROSAT* Users' Handbook" (Garching: MPE).
- Clocchiatti A., *et al.* 1997, *ApJ*, 483, 675
- Condon J. J., Condon M. A., Gisler G., Puschell J. J., 1982, *ApJ*, 252, 102
- Condon J. J., Yin Q. F., 1990, *ApJ*, 357, 97
- Conti P. S., 1991, *ApJ*, 377, 115
- Contini T., Davoust E., Considère S., 1995, *A&A*, 303, 440
- David L. P., Jones C., Forman W., 1992, *ApJ*, 388, 92
- Fabbiano G., Feigelson E., Zamorani G., 1982, *ApJ*, 256, 397
- Fabbiano G., Kim D.-W., Trinchieri G., 1992, *ApJS*, 80, 531
- Fabian A. C., Terlevich R. J., 1996, *MNRAS*, 280, L5
- Forbes D. A., Norris R. P., 1998, *MNRAS*, 300, 757
- Forbes D. A., Ward M. J., 1993, *ApJ*, 416, 150
- Ghosh S. K., Verma R. P., Rengarajan T. N., Das B., Saraiya H. T., 1993, *ApJS*, 86, 401
- Helou G., Khan I. R., Malek L., Boehmer L., 1988, *ApJS*, 68, 151
- Hjelm M., Lindblad P. O., 1996, *A&A*, 305, 727
- Hunter D. A., Gillet F. C., Gallagher J. S., Rice W. L., Low F. J. 1986, *ApJ*, 303, 171
- Irwin M., 1992, *Gemini*, 37, 1
- Iwasawa K., Fabian A. C., Ueno S., Awaki H., Fukazawa Y., Matsushita K., Makishima K., 1997, *MNRAS*, 285, 683
- Iyomoto N., Makishima K., Fukazawa Y., Tashiro M., Ishisaki Y., 1997, *PASJ*, 49, 425
- Komossa St., Schulz H., 1998, *A&A*, 339, 345
- Kristen H., Jörsäter S., Lindblad P. O., Boksenberg A., 1997, *A&A*, 328, 483
- Lamer G., Brunner H., Staubert R., 1996, *A&A*, 311, 384
- Maccacaro T., Wolter A., McLean B., Gioia I. M., Stocke J. T., Della Ceca R., Burg R., Faccini R., 1994, *Astrophys. Lett.*, 29, 267
- Maiolino R., Rieke G. H., 1995, *ApJ*, 454, 95
- Marcaide J. M., *et al.* 1992, *A&A*, 258, 295
- Marshall F. E., *et al.* 1993, *ApJ*, 405, 168
- Mas-Hesse J. M., Rodriguez-Pascual P. M., Sanz Fernández de Córdoba L., Mirabel I. F., Wamsteker W., Makino F., Otani C., 1995, *A&A*, 298, 22
- Matt G., Piro L., Antonelli L. A., Fink H. H., Meurs E. J. A., Perola G. C., 1994, *A&A*, 292, 13
- Moran E. C., Lehnert M. D., 1997, *ApJ*, 478, 178
- Muxlow T. W. B., Pedlar A., Holloway A. J., Gallimore J. F., Antonucci R. R. J., 1996, *MNRAS*, 278, 854
- Nagase F., 1989, *PASJ*, 41, 1
- Narayan R., 1996, *ApJ*, 462, 136
- Phillips A. C., Conti P. S., 1992, *ApJ*, 395, L91
- Predehl P., Trümper J., 1994, *A&A*, 290, L29
- Ptak A., Serlemitsos P., Yaqoob T., Mushotzky R., 1998, *ApJ*, (in press)
- Read A. M., Ponman T. J., Strickland D. K., 1997, *MNRAS*, 286, 626
- Saikia D. J., Pedlar A., Unger S. W., Axon, D. J., 1994, *A&A*, 270, 46
- Sandage A., Tammann G. A., 1981, *A Revised Shapley-Ames Catalogue of Bright Galaxies*. Carnegie Inst. of Washington.
- Sandqvist A., Jörsäter S., Lindblad P. O., 1995, *A&A*, 295, 585
- Schlegel E. M., 1995, *Rep. Prog. Phys.*, 58, 1375
- Shields J. C., Filippenko A. V., 1988, *ApJ*, 332, 55
- Simpson C., Forbes D. A., Baker A. C., Ward M. J., 1996, *MNRAS*, 283, 777
- Stark A. A., Gammie C. F., Wilson R. W., Bally J., Linke R. A., Heiles C., Hurwitz M., 1992, *ApJS*, 79, 77
- Stevens I. R., Strickland D. K., 1998, *MNRAS*, 294, 523
- Strickland D. K., Ponman T. J., Stevens I. R., 1997, *A&A*, 320, 378
- Strickland D. K., Stevens I. R., 1998, *MNRAS*, 297, 747
- Telesco C. M., Becklin E. E., Wynn-Williams C. G., Harper D. A., 1984, 282, 427
- Turner T. J., Urry C. M., Mushotzky R. F., 1993, *ApJ*, 418, 653
- Turner T. J., George I. M., Nandra K., Mushotzky R. F., 1997, *ApJS*, 113, 23
- Ueno S., Mushotzky R. F., Koyama K., Iwasawa K., Awaki H., Hayashi I., 1994, *PASJ*, 46, L71
- van Dyk S. D., Weiler K. W., Sramek R. A., Panagia N., 1993, *ApJ*, 419, L69
- Véron P., Lindblad P. O., Zuiderwijk E. J., Véron M. P., Adam G., 1980, *A&A*, 87, 245
- Ward M. J., 1988, *MNRAS*, 231, 1P
- Wilson A. S., Elvis M., Lawrence A., Bland-Hawthorn J., 1992, *ApJ*, 391, L75
- Wunderlich E., Wielebinski R., Klein U., 1987, *A&AS*, 69, 487
- Xue S.-J., Otani C., Mihara T., Cappi M., Matsuoka M., 1998, *PASJ*, 50, 519